J Mater Sci (2010) 45:3626–3634
DOI 10.1007/s10853-010-4408-5

Microstructure evolution of thixomolding AZ91D magnesium alloy during heat treatment

Li-jing Yang · Ying-hui Wei · Li-feng Hou

Received: 30 October 2009 / Accepted: 11 March 2010 / Published online: 25 March 2010

Abstract The microstructure evolution of thixomolding AZ91D magnesium alloy during heat treatment was investigated by means of SEM, XRD, and Vickers hardness measurement. The thixomolding AZ91D alloy has faster β phase dissolution kinetics in comparison with the HPDC alloy at 415 °C solution treatment. Both the discontinuous precipitation and the continuous precipitation were observed during aging treatment. The thixomolding specimen exhibited an accelerated age-hardening kinetics in comparison with the HPDC specimen.

Introduction

Magnesium is the lightest of all metals used as the basis for structural alloys. Mg alloys have the high potential for improving fuel efficiency and reducing CO_2 emission because of their high specific strength, high thermal conductivity, and good electromagnetic shielding characteristics, etc. [1, 2]. They are widely used in automobile and aircraft industries. But Mg alloys have low strength and ductility compared to aluminum alloys [3]. Mg alloy parts are mainly formed by high pressure die-casting (HPDC) [4, 5]. However, HPDC Mg components suffer lower engineering performance due to the existence of inherent defects, such as porosities, hot cracks, and oxide inclusions [6], which limited the extensive application of the Mg alloys. Many researchers are committed to exploring ways to improve the performance of the Mg alloy [7, 8]. Semi-solid processing is a relatively new method for processing Mg alloys in the semi-solid state at a temperature between the liquidus and the solidus to obtain near net shaped products [9]. Thixomolding, as a developing technology in semi-solid metal processing and a revolutionary new process for net-shape parts in one step in a single machine, has drawn considerable attention in recent years [10]. The thixomolding offers advantages such as extremely low porosities, finer and more uniform microstructures, and enhanced mechanical properties. Therefore, it can be heat treated which can open up new opportunities for Mg die-casting in high-stressed applications.

Previous studies have been extensively carried out on kinetics and mechanisms of the β-$Mg_{17}Al_{12}$ precipitates for AZ91 Mg alloy [11–14]. The formation of precipitate depleted zones (PDZs) near grain boundaries (GBs) was found in solution treated as well as in aged samples. The formation of PDZs is known as detrimental to the material since they may affect the mechanical and corrosion properties of the alloy [15]. Although there are several works studied the microstructure evolution of Mg alloy produced by semi-solid processes during heat treatment, there are rare reports concerning on the thixomolding Mg alloy. It is well known that different casting processes will result in a variation of the microstructure, which could influence dissolution and precipitation kinetics during subsequent heat treatment. This work systematically studied the microstructure evolution of the thixomolding AZ91D Mg alloy during heat treatment. More detailed analysis on the dissolution and precipitation kinetics during heat treatment has been done.

Experimental

The samples for this experiment were cut from the components manufactured by a JLM280-MG2E thixomolding

L. Yang · Y. Wei (✉) · L. Hou
College of Materials Science and Engineering, Taiyuan University of Technology, Taiyuan 030024, China
e-mail: yhwei@public.ty.sx.cn

L. Yang
e-mail: lijing.820228@163.com

Table 1 Chemical compositions of the specimen used in the study (mass%)

	Al	Zn	Mn	Si	Cu	Ni	Fe	Be	Mg
Specimen	9.21	0.84	0.1924	0.0387	0.0046	0.0007	0.0013	0.0009	Bal
ASTM	8.5–9.5	0.45–0.9	0.17–0.40	<0.08	<0.025	<0.001	<0.004	5–15 ppm	Bal

machine which equipped with a mobile phone housing mold in practice. The mold was preheated to 220 °C and the injection pressure was 30 MPa. The composition of the commercial Mg alloy AZ91D used in the experiment is shown in Table 1. The samples were about 0.8 mm in thickness. The solidus and liquidus temperatures reported are 468 and 598 °C, respectively, for the AZ91D alloy [16].

At the same time, a high pressure die cast (HPDC) AZ91D Mg alloy component was fabricated in a hot-chamber die-casting machine (Toshiba, 150t) with the same mold the thixomolding machine used above. The sample produced by the HPDC was used for comparison.

The AZ91D Mg alloy samples, produced by the thixomolding and the HPDC processes, respectively, were subjected to subsequent heat treatment. According to the Mg–Al binary phase equilibrium diagram, the solution treatment was carried out at 415 °C for up to 24 h (T4) in air with the protection of MgO powder. The samples were then quenched in water and aged at 216 °C for ranging from 0 to 90 h (T6).

An ECLIPSE-L150 NIKON optical microscope (OM) and a JSM-6700F scanning electron microscope (SEM) equipped with energy dispersive spectroscopy (EDS) were used to observe and analyze microstructure evolution of the specimens in different states. The specimens for the OM and SEM observation were cold mounted in self-curing resin, then polished mechanically and etched in an aqueous solution of 60 vol.% ethylene glycol, 20 vol.% acetic acid, and 1 vol.% concentrated HNO_3.

The age-hardening response and the hardness change during solution treatment were determined by Vickers hardness measurements using a load of 48 N, and the duration of loading was 15 s. No fewer than five indentations were averaged for each hardness value reported here.

Results

As-cast microstructure

The microstructures of the thixomolding and the HPDC AZ91D Mg alloy are shown in Fig. 1. The microstructure of the HPDC alloy is fine (Fig. 1a, b), and consists of two

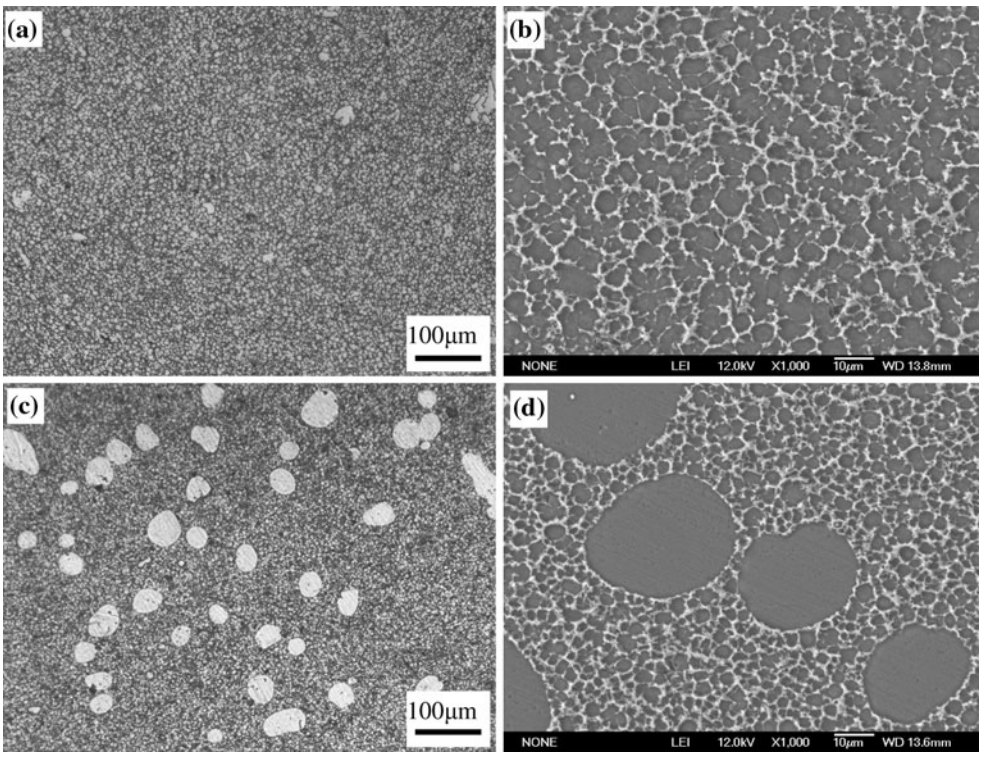

Fig. 1 Metallographical/SEM morphologies of the **a**, **b** HPDC specimen; **c**, **d** thixomolding specimen

phases, the primary α-Mg and the eutectics (α-Mg+β-$Mg_{17}Al_{12}$). Some primary α-Mg dendrites also exist. The average grain size of the primary α-Mg is roughly 6.1 μm by quantitative metallography.

The typical microstructure of the as-cast AZ91D alloy specimen produced by the thixomolding process can be described as equiaxed unmelted α-Mg globules dispersed in a continuous matrix of secondary solidified fine α-Mg and eutectics (α-Mg+β-$Mg_{17}Al_{12}$) (Fig. 1c, d). The diameters of the unmelted α-Mg globules are ranged from 30 to 60 μm. The fine secondary α-Mg grain is surrounded by a network of eutectics, which is a mixture of α-Mg and an intermetallic compound β-$Mg_{17}Al_{12}$, and the eutectics mixture distributed between the spaces of α-Mg grains. The average grain size of the secondary α-Mg is roughly 3.5 μm.

XRD analysis indicates that there is no difference in phases between the two alloy specimens. The phases in the thixomolding AZ91D alloy specimen are identified to be α-Mg solid solution and β-$Mg_{17}Al_{12}$ intermetallic compound, as shown in Fig. 2.

Response to solution treatment

Figure 3 shows the dependence of the hardness on the solution times at the same solution temperature for the two AZ91D Mg alloy specimens. The hardness values measured are observed to decrease with the solution time prolonged for both the specimens investigated. The first point of each curve in the Fig. 3 is the hardness value in the as-cast state, and the initial hardness of the thixomolding specimen is higher. It can be seen that the hardness decreases faster for the thixomolding specimen than that of the HPDC specimen when the solution time is no less than 10 h, especially at the early stage of the solution treatment (0–0.25 h). The hardness of the thixomolding specimen decreases about 19.6%, which indicates that the dissolution rate of the β-$Mg_{17}Al_{12}$ phase in the thixomolding specimen

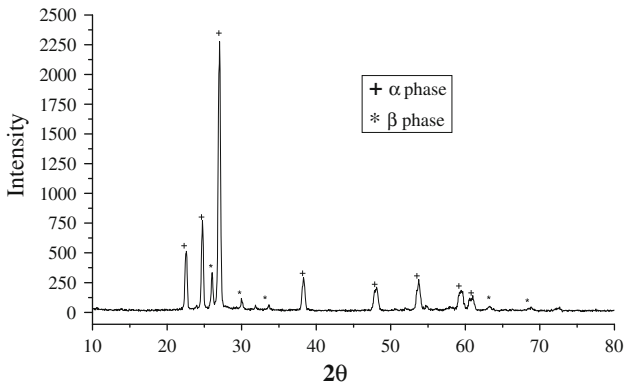

Fig. 2 X-ray diffraction patterns of the thixomolding specimen

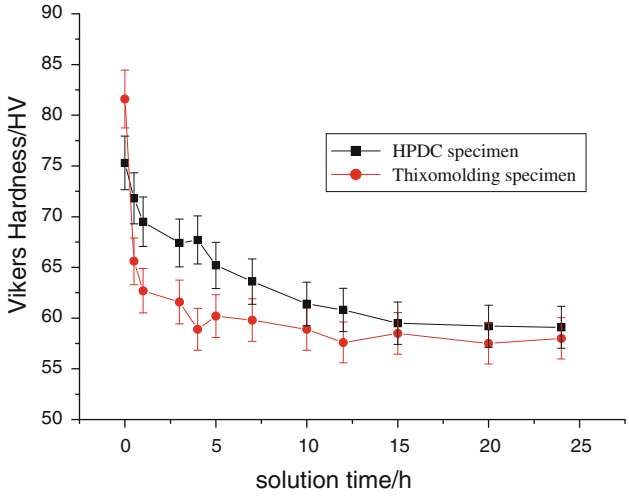

Fig. 3 Variation of the Vickers hardness of the AZ91D alloys, produced by the HPDC and the thixomolding, respectively, against time during solution treatment

is faster. The hardness value for the thixomolding specimen reaches gradually a steady state when solution treated for 12 h, while the HPDC specimen does for about 15 h. The specimens produced by the two casting processes exhibit essentially the similar hardness level after solution treatment for more than 24 h. But after 24 h heat treatment, a little of blistering occurred on the surface of die-cast AZ91D specimen. The reason for the difference in hardness during the early solution stage is that the equilibrium states and the grain sizes of the two Mg specimens are different.

XRD analysis reveals that the β-$Mg_{17}Al_{12}$ phase has completely dissolved into the α-Mg solid solution after 24 h solution treatment at 415 °C, resulting in a single-phase microstrcuture, as shown in Fig. 4.

The microstructure evolution of the thixomolding AZ91D specimen during solution treatment is shown in

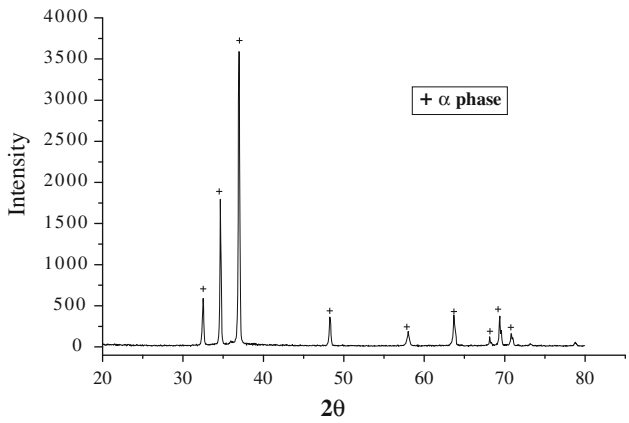

Fig. 4 X-ray diffraction patterns of the thixomolding specimen after solution treatment (T4) for 24 h

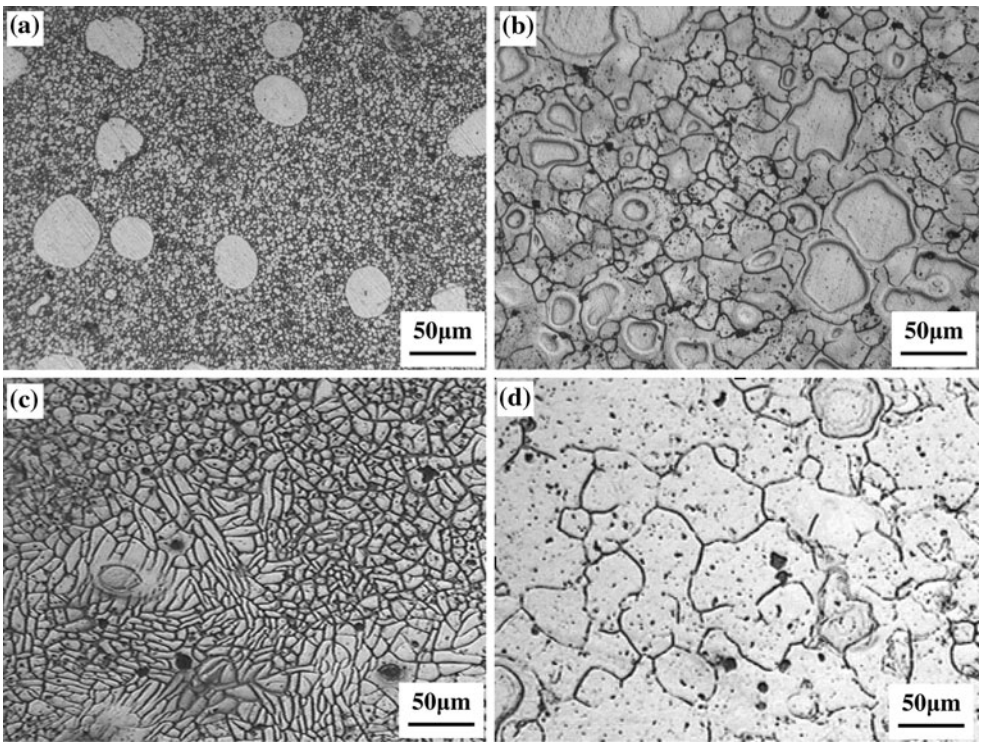

Fig. 5 Optical micrograph showing the microstructure of the thixomolding specimen after solid solution treatment (T4): **a** as-cast, **b** 0.5 h, **c** 3 h, **d** 24 h

Fig. 5. Figure 5a shows the as-cast microstructure. Some unmelted α-Mg globules distribute in the fine and homogenous eutectics matrix. After 0.5 h solution treatment, the β-$Mg_{17}Al_{12}$ phase around the secondary α-Mg has dissolved and the composition has been homogenized by diffusion. But those β-$Mg_{17}Al_{12}$ phases around the unmelted α-Mg globules are not the same (Fig. 5b). The diffusion of Al has not completely accomplished. The Al diffuses to the unmelted α-Mg globules, and results in a halo. The microstructure of the thixomolding AZ91D specimen after 3 h solution time is shown in Fig. 5c. The unmelted α-Mg globules disappeared, and the grains become fine. The β-$Mg_{17}Al_{12}$ phase has completely dissolved into the α-Mg solid solution after 3 h solution time. The grains grow obviously due to long time heat treatment, as shown in Fig. 5d. The dependence of the average grain sizes of the thixomolding and the HPDC specimens on solution times is illustrated in Fig. 6. It should be noted that the average grain size of the thixomolding specimen is focused only on the secondary α-Mg grains.

To understand the formation mechanism of the halos in Fig. 5b more clearly, the SEM observation was carried out. The microstructure morphologies under SEM observation are shown in Fig. 7. The pseudoeutectic secondary α-Mg solid solution grain is fine and relative small in size, so the β-$Mg_{17}Al_{12}$ phase around the secondary α-Mg solid solution has dissolved completely and the Al has diffused into

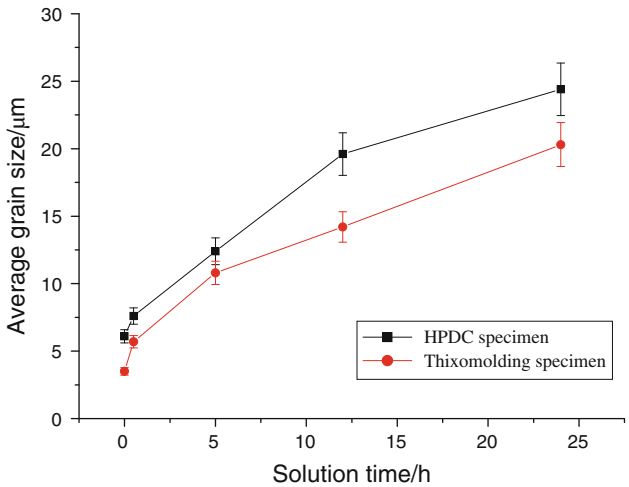

Fig. 6 The dependences of the average grain sizes of the thixomolding and the HPDC specimens on the solution times

the secondary α-Mg. But the β-$Mg_{17}Al_{12}$ phase around the unmelted α-Mg globules has not dissolved completely, the diffusion of the atoms or composition homogenization need a higher temperature or a longer period of time due to the large size of the unmelted α-Mg globule. The result of EDS line scanning shows that the content of the Al element varies with the distance from the inner of the unmelted α-Mg globule to the grain boundary, as the white line

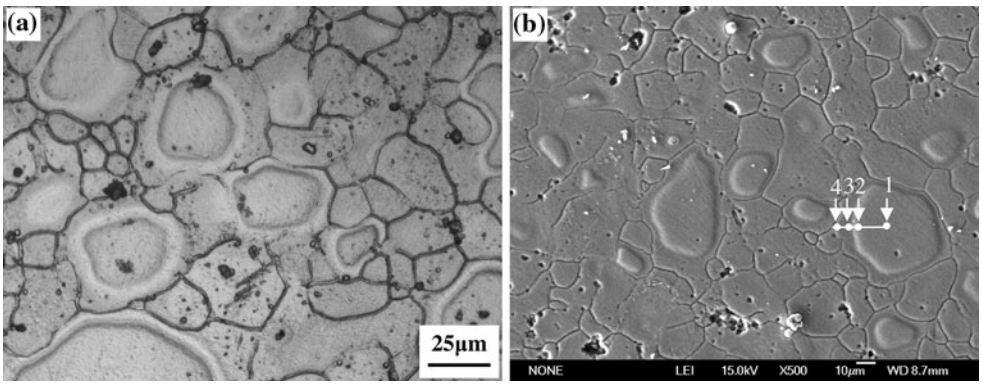

Fig. 7 Morphologies of the halos around the unmelted α-Mg globules after 0.5 h solid solution treatment: **a** optical micrograph, **b** SEM morphology

Table 2 Chemical compositions analysis of the halo present in solution treatment by EDS (mass/%)

Point	Al	Mg	O
1	3.09	96.91	0
2	3.81	96.19	0
3	5.99	94.01	0
4	8.45	85.25	6.30

showing in the picture, from point 1 to point 4. The Al contents at those positions along the white line are shown in Table 2. The Al contents at the halo (points 3 and 4) are higher than those in the unmelted α-Mg globule (points 1 and 2), but lower than that of the β-$Mg_{17}Al_{12}$ phase (The calculated value of the Al content of the β-$Mg_{17}Al_{12}$ phase is 44 mass%). This indicates that the β-$Mg_{17}Al_{12}$ phase has dissolved and the Al element diffuses from the β-$Mg_{17}Al_{12}$ phase to the unmelted α-Mg globule, so that the Al-rich halos are seen in OM and SEM micrographs at the early stage of the solution treatment. This result agrees with the result studied by Wang et al. [13].

Response to aging treatment

The age-hardening curves of the AZ91D Mg alloy specimens in two processing states, the thixomolding and the HPDC, were obtained, as shown in Fig. 8. Those specimens were subjected to solution treatment at temperatures of 415 °C and then aged at 216 °C for various periods of time. It can be seen that the hardness curves are obviously composed of three stages, which are similar to most of the precipitation-hardenable alloys. Firstly, there is an incubation period at the early stage of aging. The second is defined by a steady increase in hardness to the peak. After the peak, the hardness becomes relative steady and does not fall abruptly during aging in the experiment, which is in

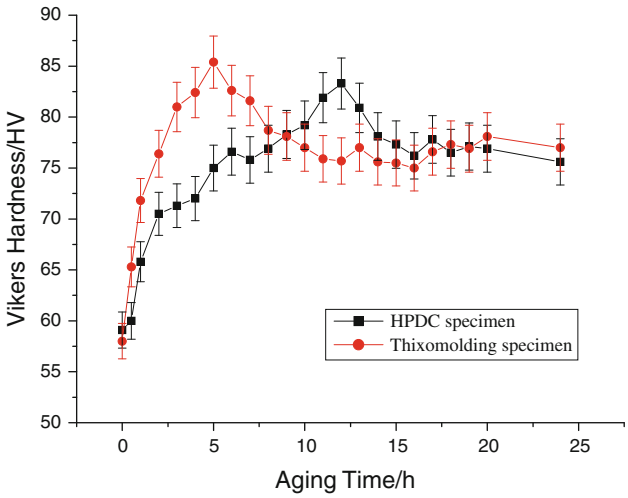

Fig. 8 Variation of the Vickers hardness of the AZ91D alloys, produced by the HPDC and the thixomolding, respectively, with aged for various times after solution treatment

contrast with the behavior of precipitation-hardenable Mg alloys [17]. The thixomolding specimen has a shorter incubation period than the HPDC specimen. This reduction in incubation period demonstrates accelerated aging kinetics of the β-$Mg_{17}Al_{12}$ phase in the thixomolding AZ91D alloy [13]. The hardness of the thixomolding specimen increases to a maximum value when aged for 5 h, while the HPDC specimen reaches the peak at about 12 h. This indicates that there is an accelerated age-hardening response at this aging temperature for the thixomolding specimen.

Figure 9 shows the microstructure evolution of the AZ91D alloy specimen processed by the thixomolding at various aging stages, that is, under-aged, peak-aged and over-aged. It can be obviously seen that the β-$Mg_{17}Al_{12}$ phases with coarse lamellar initiate preferentially at grain boundaries by discontinuous precipitation (DP), and grow

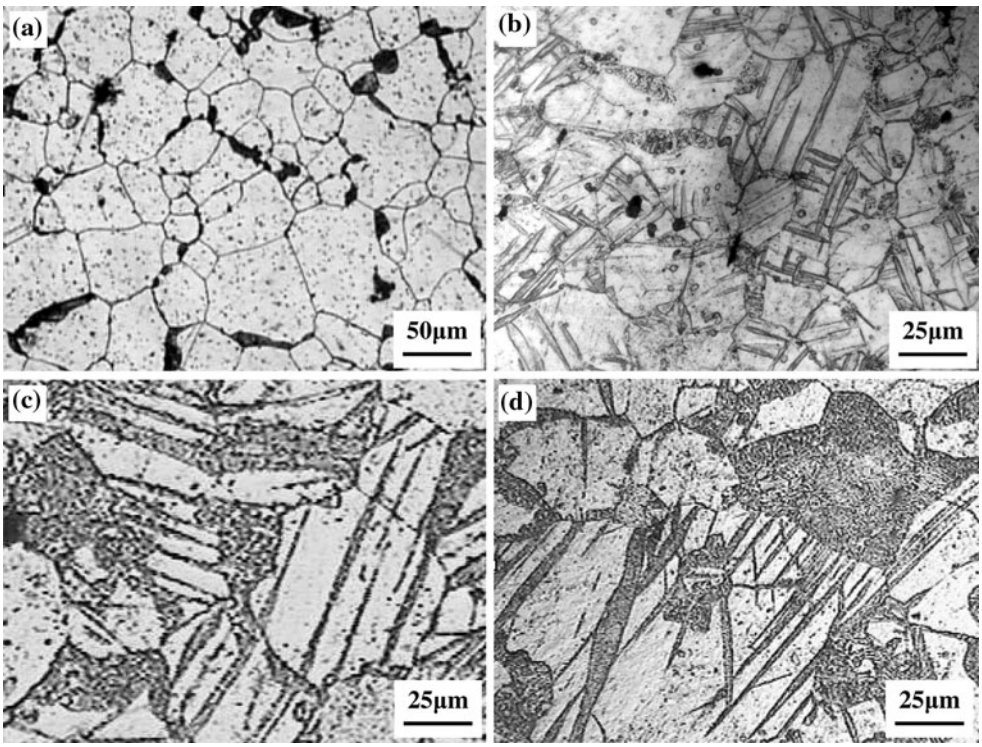

Fig. 9 Optical micrographs showing the microstructure of the thixomolding specimen after aging treatment (T_6): **a** 0.25 h, **b** 0.5 h, **c** 5 h, **d** 50 h

into the grains with aging time prolonged at the under-aged state (Fig. 9a). After aging for 0.5 h, both the DP along the grain boundaries with a lamellar morphology and continuous precipitation (CP) inside a grain with a needle-like morphology are observed (Fig. 9b). The lamellar DP cells spread from the grain boundaries into the grains, while the needle-like CPs are found to form in the remaining areas within the grains unoccupied by the DP phases. At the peak aging time, both the DP and the CP have propagated and grown. At the over-aged state, the microstructure is found to be essentially the same as the peak-aged state, containing both types of β-$Mg_{17}Al_{12}$ precipitates. But both the DP and the CP grow larger at the over-aged state (Fig. 9d). With the aging time prolonged, the DP ceases and the CP is found to form in the remaining regions of the grains where have not been occupied by the DP.

The SEM morphologies of the β-$Mg_{17}Al_{12}$ phase precipitation during the early stage are shown in Fig. 10 in greater detail. It indicates that a lamellar grows from the grain boundaries into the grain interior, which is a typical morphology for the DP of the β-$Mg_{17}Al_{12}$ phase. Two types of precipitates are clearly seen in Fig. 10b, the DP lamellas growing initially from grain boundaries into the grain and the needle-like CP forming inside the α-Mg grains.

Discussion

Dissolution of β-$Mg_{17}Al_{12}$ phase and grain coarsening during solution treatment

The specimens fabricated by the thixomolding and the HPDC were both solution treated at 415 °C for 24 h. With the solution time prolonged, the hardness values of both the specimens decreased, as shown in Fig. 3. The main reason for this phenomenon is that the β-$Mg_{17}Al_{12}$ phase dissolves into the matrix α-Mg to form supersaturated solid solution (SSS). This SSS is low in hardness, which makes the hardness of the thixomolding specimen decrease rapidly at the beginning of the solution treatment. After 3 h treatment, the hardness value tends to be stable. That is because at the early stage, there are plenty of β-$Mg_{17}Al_{12}$ phase, the concentration fluctuation of Al element between the α-Mg and β phase is large, so the diffusion of Al is fast, this results in the fast dissolution of β phase. After 3 h solution, the diffusion of Al between the α-Mg and β phase maintains a dynamic equilibrium, then a small change in hardness is exhibited until the β-$Mg_{17}Al_{12}$ phase completely dissolves into the α-Mg solid solution, but the grains obviously coarsen, as shown in Fig. 6. The volume fraction of the β-$Mg_{17}Al_{12}$ was measured by quantitative metallography, as shown in Fig. 11. It can be seen that, the β phase dissolves quite quickly in the both

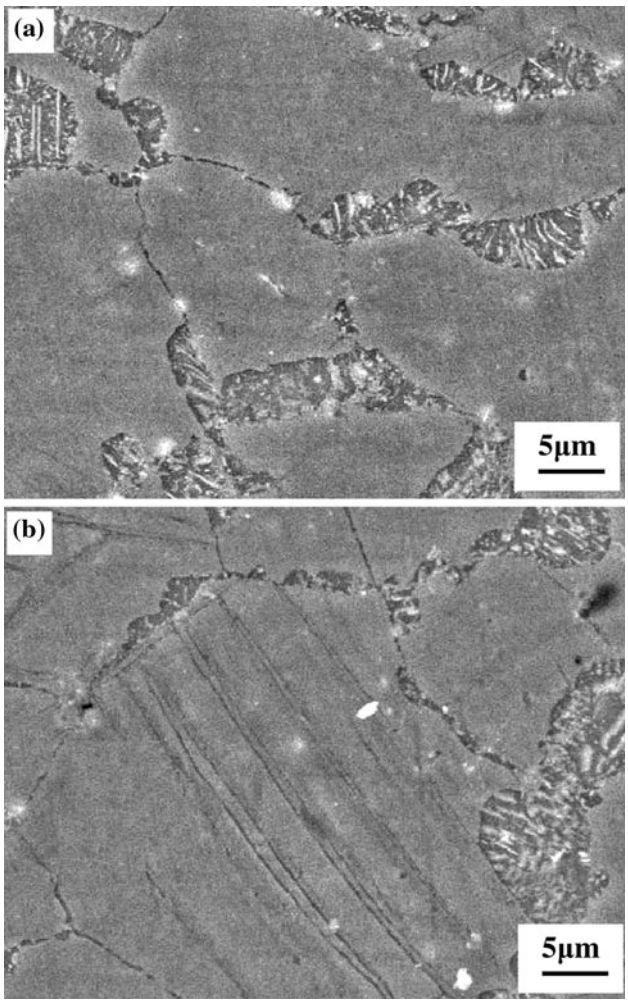

Fig. 10 SEM morphologies of the thixomolding specimen after aging treatment (T_6): **a** 0.25 h, **b** 5 h

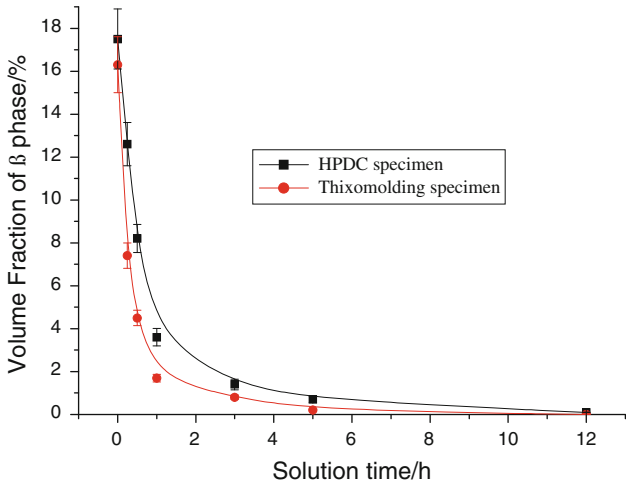

Fig. 11 Dependence of the volume fraction (%) of the β-$Mg_{17}Al_{12}$ phase on solution times (h) during the solution treatment (T4) at 415 °C

alloys. The volume fraction of the β phase of the thixomolding specimen decreases more rapidly than the HPDC alloys, showing faster β phase dissolution kinetics for the thixomolding AZ91D alloy in comparison with the HPDC alloy. The most possible explanation is proposed for the observed phenomenon. Initial secondary α-Mg grains in this alloy are perfectly equiaxed and fine, the grain boundaries are easily penetrated by diffusion. This will speed up the dissolution of the β phase.

Precipitation of the β-$Mg_{17}Al_{12}$ phase during aging

In Mg–Al alloys, the β-$Mg_{17}Al_{12}$ phase is of BCC crystal structure, and the lattice parameter is 1.056 nm [18]. During aging, the β-$Mg_{17}Al_{12}$ phase precipitates out from the SSS by two mechanisms, the DP and the CP. The resultant aging microstructure is the competition result of the DP and the CP, which are different in the rate of nucleation and growth [19]. Generally speaking, for AZ91D alloy, the DP occurs preferentially along the grain boundaries at the early stage. The cellular growth of alternating layers of the β-$Mg_{17}Al_{12}$ phase and near-equilibrium Mg matrix in the DP regions stops relative early in the precipitation process, with the CP forming in the remaining regions of the matrix grains that have not been occupied by the DP [18]. Both of these two categories phases precipitate from the Mg matrix directly to a coarsely dispersed, equilibrium precipitate β, without the appearance of Guinier–Preston (GP) zones or intermediate precipitates [20].

In this work, the lamellar DP initiates at the grain boundaries and grows perpendicular to the boundaries, as shown in Fig. 9. Once the DP is formed, it will not change in the morphology significantly. It only grows outward to consume regions which are not occupied by other precipitates. Quantitative metallographies show that the growth of the DP has declined greatly after aged for 5 h, which should be attributed to the CP taking place at that time. For the CP, there are three different types of habits, and each type associates with a different matrix/precipitate orientation [17].

It should be noted that, some annealing twins can be observed after aging for 0.5 h. The driving force of the annealing twins may come from the residual microstructure stresses left during thixomolding process.

The morphologies and structures of the needle-like CPs occurring in this work are similar with the needle-like phase (NLP) which studied by Wei et al. [21]. According to the proposal of Wei, this NLP is of dhcp structure. Orientation relationship between the NLP and the parent has been determined as $(0001)_{NLP}\|(10\bar{1}0)_{parent}$, and $[0001]_{NLP}\|[10\bar{1}0]_{parent}$ or $[2\bar{1}\bar{1}0]_{NLP}\|[2\bar{1}\bar{1}3]_{parent}$.

In the age-hardening curves, the thixomolding specimen exhibits accelerated age-hardening kinetics in comparison

with the HPDC specimen. A faster response to solution treatment and an accelerated dissolution of the β-$Mg_{17}Al_{12}$ phase during solution at 415 °C have also been observed in the present study. According to the proposals of Huang [14], there is a competitive relationship between the CP and the DP in an intricate manner during heat treatment due to the difference in nucleation and growth rates. Most of the areas are occupied by the DP, which abides by the nucleation mechanism proposed by Fournelle and Clark (F–C). Nucleation rate per unit area of grain boundary for F–C mechanism, $I_{s,FC}$, was proposed [22] as

$$I_{s,FC} \propto \nu \exp\left[-\frac{E}{RT}\right]\frac{\gamma V_m}{d}P_{nuc,FC} \quad (1)$$

where ν is the vibration frequency of the grain boundary considered as membrane, E the activation energy for vibration of the membrane, γ surface energy, V_m the molar volume, $\gamma V_m d^{-1}$ the capillarity energy responsible for the first displacement of the boundary, and $P_{nuc,FC}$ the probability that the displacement of the grain boundary induced by capillarity forces will allow a DP nodule to nucleate. As ν is proportional to d^{-1} and assuming that the dependence of $P_{nuc,FC}$ on d is small, the $I_{s,FC}$ is proportional to d^{-2}, the $I_{s,FC}$ and d^2 has an inversely proportional relationship, that is to say, the larger the grain size is, the lower the nucleation rate will be. In this work, the grain size of the thixomolding AZ91D specimen after 24 h solution treatment at 415 °C is smaller than that of the HPDC specimen, so the nucleation rate of the DP is faster, and the precipitation rate is definitely faster. These result in a higher increase rate in hardness. At last, the thixomolding specimen exhibits accelerated age-hardening kinetics in comparison with the HPDC specimen.

The growth kinetics of the DP and dissolution reactions in Mg-rich Al alloys have been investigated by Gust et al. [23]. The volume fraction of the regions transformed by the DP reaction, the reaction front velocity, the interlamellar spacing and the average composition of the solute-depleted (Mg) lamellae determined as a function of the temperature and solute content were found to show the behavior typical for the discontinuous precipitation reaction. The grain boundary diffusivities calculated using the Petermann–Hornbogen equation were found to be in the range from 1×10^{-23} to 1×10^{-17} m^3/s. These values convincingly showed that the transport of the solute atoms during the DP and discontinuous dissolution reactions in Mg–Al alloys is governed by grain boundary diffusion.

Conclusions

(1) The as-cast microstructure of the AZ91D Mg alloy specimen processed by thixomolding is comprised of equiaxed unmelted α-Mg globules, secondary solidified α-Mg and eutectics (α-Mg+β-$Mg_{17}Al_{12}$). The diameters of the unmelted α-Mg globules are ranged from 30 to 60 μm, and the average grain size of the secondary α-Mg is roughly 3.5 μm. The microstructure of the HPDC specimen is more uniform and the average grain size is roughly 6.1 μm.

(2) The AZ91D Mg alloy specimen processed by thixomolding exhibits a faster β phase dissolution rate than the HPDC alloy at 415 °C solution treatment. The Al-rich halos have been seen at the early stage of the solution treatment because of Al diffusing from the β phase to the unmelted α-globules. The thixomolding AZ91D alloy has faster β phase dissolution kinetics in comparison with the HPDC alloy. The reason is that, initial secondary α-Mg grain in the thixomolding specimen is equiaxed and fine, which makes the dissolution rate of the β-$Mg_{17}Al_{12}$ faster.

(3) The hardness of the AZ91D alloy specimen processed by the thixomolding reaches the peak after aged for 5 h, while the HPDC specimen takes 12 h. Both the DP and the CP of the β-$Mg_{17}Al_{12}$ are observed during aging treatment. The thixomolding specimen exhibits an accelerated age-hardening kinetics in comparison with the HPDC specimen.

Acknowledgements The authors gratefully acknowledge the National Natural Science Foundation, People's Republic of China, the Science and Technology Project of Taiyuan City (08121018), the Shanxi Province Foundation for Returned Scholars, the Shanxi Province Young Subject-Leader Foundation, and the Innovative Project for Outstanding Post-graduate of Shanxi Province (20093007) for providing funding in support of this work.

References

1. Chino Y, Sassa K, Mabuchi M (2009) J Mater Sci 44:4593. doi:10.1007/s10853-009-3700-8
2. Wei Y-h, Hou L-f, Yang L-j, Xu B-s (2009) J Mater Process Technol 209:3278
3. Hou L-f, Wei Y-h, Liu B-s, Xu B-s (2008) J Mater Sci 43:4658. doi:10.1007/s10853-008-2668-0
4. Hakamada M, Shimizu K, Yamashita T, Watazu A, Saito N, Iwasaki H (2010) J Mater Sci 45:719. doi:10.1007/s10853-009-3990-x
5. Park JP, Kim MG, Yoon US, Kim WJ (2009) J Mater Sci 44:47. doi:10.1007/s10853-008-3130-z
6. Du X, Zhang E (2007) Mater Lett 61:2333
7. Wang S, Kang SB, Cho JH (2009) J Mater Sci 44:5475. doi:10.1007/s10853-009-3762-7
8. Figueiredo RB, Langdon TG (2009) J Mater Sci 44:4758. doi:10.1007/s10853-009-3725-z
9. Zhao Z, Chen Q, Wang Y, Shu D (2009) Mater Sci Eng A 506:8
10. Zhang YF, Liu YB, Cao ZY, Zhang QQ, Zhang L (2009) J Mater Process Technol 209:1375
11. Czerwinski F (2003) Scripta Mater 48:327
12. Tamura Y, Kida Y, Tamehiro H, Kono N, Soda H, McLean A (2008) J Mater Sci 43:1249. doi:10.1007/s10853-007-2276-4
13. Wang Y, Liu G, Fan Z (2006) Acta Mater 54:689

14. Huang J, Yu H, Li Y, Hua C, He J, Zhang J (2009) Mater Des 30:440
15. Shepelev D, Bamberger M, Katsman A (2009) J Mater Sci 44:5627. doi:10.1007/s10853-009-3793-0
16. Czerwinski F (2002) Acta Mater 50:3265
17. Lai WJ, Li YY, Hsu YF, Trong S, Wang W (2009) J Alloys Comp 476:118
18. Celotto S (2000) Acta Mater 48:1775
19. Duly D, Simon JP, Brechet Y (1995) Acta Metall Mater 43:101
20. Celotto S, Bastow TJ (2001) Acta Mater 49:41
21. Wei Y-h, Hou L-f, Xu B-s (2009) J Alloys Comp 467:130
22. Duly D, Brochet Y, Chenal B (1992) Acta Metall Mater 40:2289
23. Bradai D, Kadi-Hanifi M, Zieba P, Kuschke WM, Gust W (1999) J Mater Sci 34:5331. doi:10.1023/A:1004753122411